J. Math. Biol. (1994) 33: 139–161

Journal of Mathematical Biology

Translating stochastic density-dependent individual behavior with sensory constraints to an Eulerian model of animal swarming

Daniel Grünbaum*

Department of Zoology, University of Washington, Seattle, WA 98195, USA

Received 13 January 1993; received in revised form 14 February 1994

Abstract. Density-dependent social behaviors such as swarming and schooling determine spatial distribution and patterns of resource use in many species. Lagrangian (individual-based) models have been used to investigate social groups arising from hypothetical algorithms for behavioral interactions, but the Lagrangian approach is limited by computational and analytical constraints to relatively small numbers of individuals and relatively short times. The dynamics of "group properties", such as population density, are often more ecologically useful descriptions of aggregated spatial distributions than individual movements and positions. Eulerian (partial differential equation) models directly predict these group properties; however, such models have been inadequately tied to specific individual behaviors. In this paper, I present an Eulerian model of density-dependent swarming which is derived directly from a Lagrangian model in which individuals with limited sensing distances seek a target density of neighbors. The essential step in the derivation is the interpretation of the density distribution as governing the occurrence of animals as Poisson points; thus the number of individuals observed in any spatial interval is a Poisson-distributed random variable. This interpretation appears to be appropriate whenever a high degree of randomness in individual positions is present. The Eulerian model takes the form of a nonlinear partial integro-differential equation (PIDE); this equation accurately predicts statistically stationary swarm characteristics, such as expected expected density distribution. Stability analysis of the PIDE correctly predicts transients in the stochastic form of the aggregation model. The model is presented in one-dimensional form; however, it illustrates an approach that can be equally well applied in higher dimensions, and for more sophisticated behavioral algorithms.

* *Present address*: Department of Mathematics, University of British Columbia, Vancouver, British Columbia, 6T 1Y4, Canada

Key words: Aggregation – Density-dependent behavior – Animal distributions

1 Introduction

Social groups of animals such as schools and swarms are formed and maintained by numerous interactions between individuals, each of which continually responds to neighboring animals according to characteristic sets of behaviors. Individual behaviors ultimately result in group-level properties, which determine the success of a group in fulfilling such functions as detecting prey, avoiding predators, and finding mates. Group properties include inter-individual spacing, orientational polarity of group members, and the integrity of the group in the face of external disturbances. These properties occur mainly at "local" spatial scales and may be observed within relatively short time intervals. Other effects of social aggregative behavior, however, operate at much larger spatial and temporal scales. This category may include such ecologically important effects as the distribution of group sizes within a population, segregation of individuals by size, age, or sex, and long-range foraging or migratory movement patterns.

The distinction between local and ecological spatio-temporal scales is paralleled by two approaches to describing and modelling animal distributions, the **Lagrangian** and **Eulerian** approaches. Lagrangian models (also known as **individual-based** or **stochastic** models) are a class of models in which the trajectories of individual animals are calculated, according to equations that may incorporate both physical laws (e.g. conservation of momentum) and elements of social behavior (such as attraction to, repulsion from, or tendency to align with neighbors). Theoretical investigations of compactness, polarization, or cohesion of groups have typically employed Lagrangian models to explore the consequences of particular behavioral algorithms, because complicated behavioral rules can be implemented directly and because the resulting individual positions are directly comparable to observations of real schools and swarms. Lagrangian models of social aggregation are thus well-suited to identify possible constraints and trade-offs in attaining desirable local group properties. However, they are generally restricted by computational requirements to relatively small numbers of individuals for relatively short times. This makes the Lagrangian approach impractical for understanding the ecological-scale distributional effects of social aggregation behaviors.

Eulerian aggregation models (also known as **continuum** or **population** models) represent animal positions in the form of a density distribution and a partial differential equation which governs the density flux (e.g. Kawasaki 1978, Cohen and Murray 1981, Alt 1985, Turchin 1989, Pfistner and Alt 1990). Eulerian models can efficiently describe distributions of large numbers of animals over ecological time and space scales. However, since individual animals are not represented in Eulerian models, it is not possible to directly implement social interactions. Instead, an expression for the density flux must

be derived from a Lagrangian-type social behavioral algorithm. To date, most Eulerian descriptions of social behaviors are based on heuristic interpretations of Lagrangian algorithms, because procedures for performing this derivation rigorously have not been fully developed.

In constrast to density-independent behaviors such as chemotaxis, fluxes arising from social behaviors are inherently non-linear. Social behaviors require a more complete and specialized interpretation of "density" than asocial behaviors. This can be shown with a general mathematical expression of an animal's social responses. Let the social behavioral decision of an individual at position x (which may have consequences such as changes if speed or heading) be formalized as $f(x, t, v_1, v_2, \ldots, v_M)$, where v_i is the number of individuals observed at time t in one of M spatial intervals, $\boldsymbol{d}_i$. Virtually any social algorithm can be expressed in this form (for example, f can be stochastic, $M \to \infty$ can be yield continuous variation in space, etc.). The decision function may be expanded in a Taylor series,

$$f(x, t, v_1, v_2, \ldots, v_M) = f(x, t, \rho_1, \rho_2, \ldots, \rho_M) + \sum_{i=1}^{M} \rho_i' \frac{\partial f}{\partial \rho_i'} + \sum_{i,j=1}^{M} \rho_i' \rho_j' \frac{\partial^2 f}{\partial \rho_i' \partial \rho_j'} + \cdots \tag{1}$$

where $\rho_i = E\{v_i\}$ is the average number of individuals in $\boldsymbol{d}_i$, $\rho_i' = v_i - \rho_i$ is the deviation from the average in a given realization, and the derivatives are evaluated at $v_i = \rho_i$ ($E\{\ \}$ denotes expected value). Calculation of the density flux requires an expression for the expected value of the decision function, $\phi(x, t) = E\{f\}$. In expanded form,

$$\phi(x, t) = f(x, t, \rho_1, \rho_2, \ldots, \rho_M) + \sum_{i,j=1}^{M} E\{\rho_i' \rho_j'\} \frac{\partial^2 f}{\partial \rho_i' \partial \rho_j'} + \cdots \tag{2}$$

In (2), non-linear behavioral terms appear in the expected decision as functions of joint probability distributions between intervals and/or higher order statistics within intervals.

These non-linear terms represent responses that are essential to many aspects of "reasonable" social behavior. For example, an isolated fish with schooling tendencies may be strongly attracted to a nearby group. If, on the other hand, the fish is not isolated but within a group of its own, attraction to the other group may be weak or absent. Thus its social responses involve non-linear interactions between numbers of neighbors observed in distinct sampling domains. Other examples include most forms of saturating responses, and of modulating and prioritizing responses to multiple neighbors based on relative proximity of orientation (Aoki 1982, Huth and Wissel 1990, 1992). To obtain an equation describing density flux, the higher order statistics must be somehow *implicit* in the density distribution, a requirement not present for density-independent behaviors, and one not addressed in most models to date.

In this paper, I present a new method for deriving an Eulerian aggregation model from a Lagrangian model in which non-linear behavioral responses are present, using as an example a simplified one-dimensional model of density-dependent swarming. The key elements of these paired Lagrangian and Eulerian models are: (*1*) an innate tendency of individuals to move towards a species-specific "target" density of neighbors; (*2*) an individual's imperfect perception of surrounding animal distributions because of limitations on the ability to detect and respond to distant neighbors; and (*3*) the stochasticity of relative positions of animals within a swarm or school, and the consequent randomness in movement decisions made in response to neighbors' positions. Specifically, I obtain the density flux by assuming that, at any given observation, individuals are distributed as a set of Poisson points governed by the density distribution. This assumption is apparently satisfied when the number of neighbors perceived by an individual has a sufficient level of random fluctuations. The resulting Eulerian model, which takes the form of a non-linear partial integro-differential equation, accurately predicts the distribution within an aggregation observed in the Lagrangian model. Linear stability analysis of the Eulerian model predicts the initial size of groups arising from unstable initial conditions.

Since this work was originally inspired by an interest in krill aggregations, the terminology used here is appropriate to aquatic organisms. The approach is, however, intended to be more generally applicable in terrestrial as well as aquatic settings.

2 Lagrangian swarming model

In this section, I present a Lagrangian model of density-dependent aggregation; I will obtain an Eulerian form of this model in the succeeding sections. The Lagrangian model calculates the spatial distribution patterns of a population of identical, idealized animals swarming in a one-dimensional domain. The social behavior displayed by model individuals has two primary features, a "sensing distance" and a "target density." Individuals are assumed to have a finite sensing distance, ζ, within which neighboring individuals can be detected and counted. Individuals have no information about other individuals distant by more than ζ. Thus, referring to (1), there are two spatial intervals which are sampled during social behavior by an animal at x, i.e., $\boldsymbol{d}_1 = [x - \zeta, x]$ and $\boldsymbol{d}_2 = [x, x + \zeta]$. The idea of a limit to the range over which interactions between individuals can occur has been used in previous Lagrangian models of schooling and swarming (e.g., Aiko 1982, Heppner and Grenander 1990, Huth and Wissel 1990, 1992). Such a limit on individuals' information-gathering abilities could constrain the range of possible group properties available to them.

I include density-dependent aggregation in the model by assuming that individuals have an intrinsic target level of population density, μ. Each individual seeks out regions with density μ by moving in the plus or minus

x-direction, according to whether $\boldsymbol{d}_1$ or $\boldsymbol{d}_2$ has more neighbors and whether the total number of detected neighbors (plus itself) is above or below the target number, $2\zeta\mu$. This behavioral algorithm is non-linear; thus, according to (2), the expected value of the decision will require higher order statistics on the number of neighbors observed in $\boldsymbol{d}_1$ and $\boldsymbol{d}_2$.

The algorithm for social behavior differs from "tendency-distance" formulations, often used in models of fish schooling, in which individuals experience attraction or repulsion from each neighbor independently as a function of the separation distance to that neighbor (e.g., Suzuki and Sakai 1973, Aiko 1982, Heppner and Grenander 1990, Warburton and Lazarus 1991). The target density formulation has several advantages in the present context. First, tendency-distance models are often written with linear responses; this omits important aspects of density-dependent dynamics. Second, the target density approach is a one-dimensional description of swarming which is more analogous to the actual three-dimensional process than a one-dimensional tendency-distance model, in that individuals are not constrained from passing one another, as they would be if they experienced strong repulsion at short separation distance (most tendency-distance models in the literature are two-dimensional). Finally, tendency-distance models typically have a continuous variation of interaction strength with separation distance and orientation. Good approximations to these models would require more than two sampling intervals, increasing the computational effort without adding to the demonstration value of the present model. Therefore, I adopt the one-dimensional target density formulation, while noting that the underlying approach also applies, with greater computational effort, in multiple dimensions and with more complicated behaviors. I also assume that spacing between animals is large compared to body length, so that any constraints on density or movement are negligible.

Movement of a model individual is the result of a time-dependent force, $F(t)$, which represents both social and asocial aspects of behavior. Individuals observe their neighbors and make social movement decisions at random times, at an average rate of λ_s. Each time an individual makes a social decision, it counts the number of individuals within the sensing distance, ζ, in the negative (v_1), and positive (v_2) x directions. This gives an estimate of $(1 + v_1 + v_2)/2\zeta$ for the local population density (including, by convention, the observing individual). An individual estimates the sign of the local gradient by comparing v_1 to v_2. If a difference between the local and the target densities exists, the individual responds by moving up or down the perceived local gradient, as appropriate. This social behavior can be expressed as decision functions,

$$\begin{aligned} f_1(v_1, v_2) &= \operatorname{sgn}(2\zeta\mu - 1 - v_1 - v_2) \,, \\ f_2(v_1, v_2) &= \operatorname{sgn}(v_1 - v_2), \text{ and} \\ f(v_1, v_2) &= f_1(v_1, v_2) f_2(v_1, v_2) \,. \end{aligned} \tag{3}$$

In (3), f_1 represents the response to seek higher or lower densities; it takes on the values 1 or -1 depending on whether there are too many or too few neighbors. f_2 represents the direction of the perceived local gradient; it has a value of 1 if more neighbors are visible on the right side than the left, and -1 if more neighbors are visible on the left side than the right. f is the resulting movement decision made according to the social behavior algorithm, with value 1 representing a decision to move to the right and -1 to move to the left. The result of a social movement decision is a force, $f\alpha$, imposed on the individual, where α is a parameter determining the magnitude of the social response.

In addition to social forces, individuals are also subject to a random, density-independent force, which is selected from a Gaussian distribution with zero mean and variance σ^2 at random intervals at an average rate of λ_r. This force can be interpreted variously as an innate tendency to move randomly, as random environmental forcing such as advection in a turbulent field, or as the deterministic behavioral response to a random environment such as feeding in a turbulently diffused food patch. Each behavioral choice replaces the force from the previous choice, whether it is a social or asocial. $F(t)$ is constant within the time intervals between choices.

In response to forces, individuals move according to a linear movement equation (see also Sakai 1973, Suzuki and Sakai 1973 and Okubo 1986),

$$m\frac{d^2x}{dt^2} + d\left(\frac{dx}{dt} - U\right) = F(t)\,. \tag{4a}$$

In (4a), x is the individual's position, m is its mass, d is a drag coefficient, and U is an advection velocity of the surrounding fluid which may vary in both time and space. This equation, while not a dynamically complete description of animal motion, illustrates that the approach I take in this paper applies to Lagrangian models in which individual position is continuous in time and space, and does not require discretization. Equation (4a) can be nondimensionalized, using the characteristic time $\tau = m/d$, length ζ, and force $m\zeta/\tau^2$, to give

$$\frac{d^2x}{dt^2} + \frac{dx}{dt} = F(t) + U\,. \tag{4b}$$

In (4b), an individual can detect neighbors within a unit sensing distance on either side, so it sees $2\mu - 1$ neighbors at the target density.

The instantaneous and time-averaged density distributions of a statistically stationary swarm formed by individuals following these behavioral rules are shown in Fig. 1a. A typical aggregation has three distinct regions of population density: an interior region of approximately uniform density, an interface region of exponentially decreasing density, and an exterior populated by a uniformly low number of individuals which have strayed from the swarm.

Although all individuals seek the same target density, μ, the density within the aggregation is substantially higher than the target. Tendency-distance

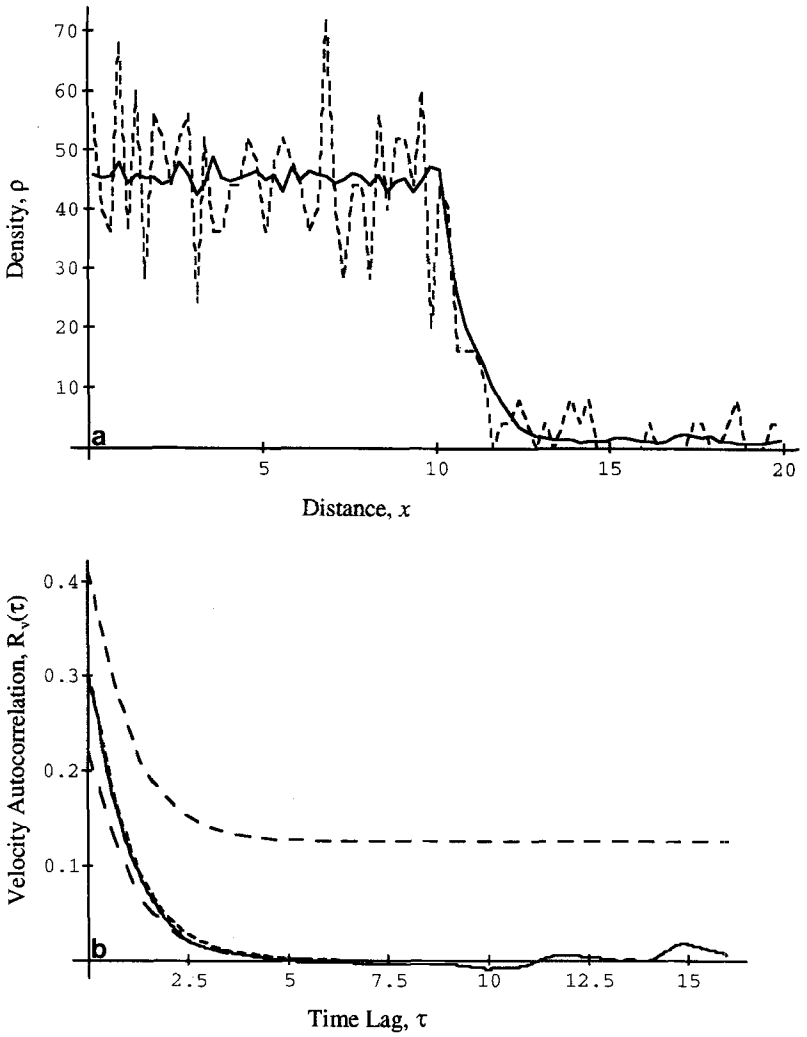

Fig. 1. **a** Instantaneous (*dashed line*) and time-averaged (*solid line*) densities of a statistically stationary aggregation formed by 512 individuals in the stochastic model. Parameters are $\lambda_r = 6.586$, $\sigma = 1.599$, $\lambda_s = \sqrt{2}$, and $\alpha = 2.0$; these correspond to $D = 1/4$, $\gamma = \sqrt{2}/4$, $\lambda = 8$, and $\Delta x_s = 1/4$. Densities are estimated within bins of size 1/4. The origin is a reflective boundary; the individuals were initially uniformly distributed around the origin at a density of 4μ. **b** Measured (*solid line*) and predicted (*dashed lines*) velocity autocorrelation, $R_v(\tau)$, averaged over all individuals. For short time lags ($\tau > 5$), the measured autocorrelation is nearly indistinguishable from the predicted autocorrelation for the interior of an aggregation (*short dashes*); this is expected, since most individuals spend most of the time in the interior. Also shown are the predicted autocorrelations for individuals whose directed forcing is consisently in one direction (*medium dashes*) and isolated individuals (*long dashes*); **c** Density variance vs. mean density for each bin. For a Poisson process, the ratio of variance to mean is one; the line of equal mean and variance is shown as a dashed line. Measured ratios are generally close to one, consistent with the Poisson process assumption. Variance in the interior of the aggregation is lower than predicted by the Poisson assumption. However, this is in a region where mean aggregation velocity is zero; the error introduced in the estimate of density fluxes should therefore be small

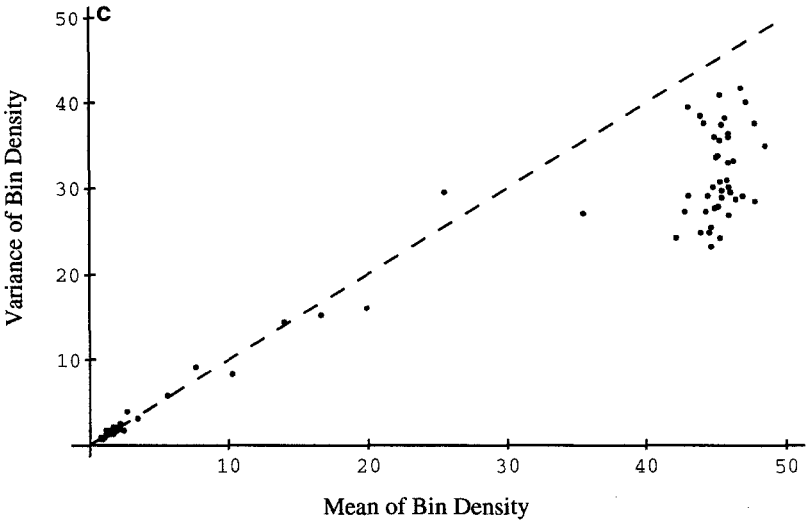

Fig. 1c

models may also display overcrowding (Warburton and Lazarus 1991). Interestingly, it appears that interior animals inside some schools of fish and krill may be stressed by overcrowding, indicating that density in these groups may also be higher than optimal for group members (Moss and McFarland 1967, Strand and Hamner 1990). These observations suggest that difficulty in regulating density within groups may be a common result of the decentralized control operating in animal aggregations.

3 Reparametrization

In this section, I find combinations of parameters from the Lagrangian model that describe the large-scale effects of the Lagrangian behaviors. In particular, the analysis in this section gives expressions for a diffusion constant and a characteristic aggregation velocity, both of which will appear in the Eulerian form of the model.

I begin by calculating the characteristic step length associated with a single behavioral choice. From (4b), an individual's position after a series of intervals, $\Delta t_j = t_{j+1} - t_j$, within which the force is constant, $F(t) = F_j$, $t_j < t < t_{j+1}$, is given by

$$x(t) - x(t_0) = \frac{dx(t_0)}{dt}(1 - e^{-\Delta t}) + U(\Delta t - (1 - e^{-\Delta t})) + \sum_{k=0}^{j-1} F_k[\Delta t_k + e^{-(t-t_{k+1})}(1 - e^{-\Delta t_k})], \quad (5)$$

where $x(t_0)$ and $dx(t_0)/dt$ are the initial position and velocity, respectively. As the time since the end of the kth interval, $t - t_{k+1}$, becomes large, the displacement, Δx_k, of an individual due to the constant force F_k on the individual in the interval Δt_k approaches the non-dimensional impulse generated within the interval,

$$\lim_{t \to \infty} \Delta x_k = F_k \Delta t_k \,. \tag{6}$$

Equation (6) gives the total distance the animal moves as a result of the behavioral choice at the start of the kth time interval, and makes it possible to calculate characteristic step sizes for social and asocial movements. Equations (5) and (6) also may be useful in estimating Lagrangian behavioral parameters for animals, using observations of step size and frequency.

In the Lagrangian model, new forces occur randomly at an average total rate of

$$\lambda = \lambda_r + \lambda_s \,, \tag{7}$$

where a fraction λ_r/λ are asocial random forces, and the remaining forces are social. Forces are chosen randomly with constant probability in time; the force duration, Δt, has a mean and mean squares (Papoulis 1984) of

$$E\{\Delta t\} = \frac{1}{\lambda}, \qquad E\{\Delta t^2\} = \frac{2}{\lambda^2}. \tag{8}$$

The expected values of square random step length, Δx_r^2, and interval at which random steps are taken, Δt_r, are, from (6),

$$\Delta x_r^2 = E\{F_r^2\}\, E\{\Delta t^2\} = \frac{2\sigma^2}{\lambda}, \quad E\{\Delta t_r\} = \frac{1}{\lambda_r} \,. \tag{9}$$

From (9), the diffusion coefficient for the expected density flux due to random forcing (Levin 1986) is

$$D = \frac{\Delta x_r^2}{2\, E\{\Delta t_r\}} = \frac{\sigma^2 \lambda_r}{\lambda^2} \,. \tag{10}$$

The average interval between directed steps and the average directed step length are

$$E\{\Delta t_s\} = \frac{1}{\lambda_s} \,, \qquad \Delta x_s = E\{|F_s \Delta t|\} = \frac{\alpha}{\lambda} \,. \tag{11}$$

A velocity, γ, characterizing the directed forcing is

$$\gamma = \frac{\Delta x_s}{E\{\Delta t_s\}} = \frac{\alpha \lambda_s}{\lambda} \,. \tag{12}$$

In (10), γ is the maximum average aggregation speed (i.e., that of an individual whose social forcing is consistently in the same direction).

In summary, the diffusion coefficient, D, the net rate of new force selection, λ, the characteristic aggregation velocity, γ, and the average directed step length, Δx_s, are Eulerian aggregation parameters which can be expressed in

terms of the original stochastic model parameters. The stochastic model parameters are also uniquely specified in terms of the Eulerian parameters,

$$\begin{aligned}
\lambda_r &= \lambda - \frac{\gamma}{\Delta x_s}, \\
\sigma &= \sqrt{\lambda D\left(1 - \frac{\gamma}{\gamma - \Delta x_s \lambda}\right)}, \\
\lambda_s &= \frac{\gamma}{\Delta x_s}, \text{ and} \\
\alpha &= \Delta x_s \lambda .
\end{aligned} \tag{13}$$

In the next two sections, these new parameters are used, together with the autocorrelation of individual velocity, to derive a continuum approximation to the stochastic aggregation model.

4 Velocity autocorrelation and power spectrum

In this section, I derive an expression for the velocity autocorrelation of an individual, from which I will infer the form of the Eulerian equation describing the flux of individuals. The velocity autocorrelation is found by application of Fourier transforms, using the power spectrum of individual forcing and the transfer function between forcing and velocity. The analysis assumes that individual velocities in a neighborhood are statistically stationary, a condition that is satisfied when the density distribution changes slowly on non-dimensional time scales of unity (the velocity relaxation time) and spatial scales of γ (the distance traveled at the maximum average rate in the velocity relaxation time).

The velocity autocorrelation, $R_v(\tau)$, is related to its power spectrum, $S_v(\omega)$, by a Fourier transform (Papoulis 1984),

$$\begin{aligned}
S_v(\omega) &= \frac{1}{\sqrt{2\pi}} \int_{-\infty}^{\infty} R_v(\tau) e^{-i\omega\tau} \, d\tau , \\
R_v(\omega) &= \frac{1}{\sqrt{2\pi}} \int_{-\infty}^{\infty} S_v(\tau) e^{i\omega\tau} \, d\omega ,
\end{aligned} \tag{14}$$

The Fourier transform of (4) gives the transfer function between force and velocity (considering now the case $U = 0$),

$$(1 + i\omega)\,\hat{v}(\omega) = \hat{F}(\omega) , \tag{15a}$$

where carets indicate transformed quantities. From (15a) it follows that the power spectrum of velocity, $S_v(\omega)$, can be obtained from the spectrum of forcing,

$S_F(\omega)$, with

$$S_v(\omega) = \frac{S_F(\omega)}{(1+\omega^2)} . \tag{15b}$$

The forcing autocorrelation, $R_F(\tau)$ is the sum of the autocorrelations of random and social forcing,

$$R_F(\tau) = R_r(\tau) + R_s(\tau) , \tag{16}$$

because the two types of forcing are uncorrelated. The random force is uncorrelated with itself at two different times unless these times lie within the same interval. The random force autocorrelation is therefore the product of the mean square forcing amplitude and the probability that two random times, τ apart, are in the same forcing interval (Papoulis 1984),

$$R_r(\tau) = \sigma^2 \frac{\lambda_r}{\lambda} e^{-\lambda|\tau|} . \tag{17a}$$

The random component of the forcing power spectrum is then

$$S_r(\omega) = \sqrt{\frac{2}{\pi}} \frac{2\sigma^2\lambda_r}{\lambda^2+\omega^2} . \tag{17b}$$

As in random forcing, the autocorrelation of the social forcing contains a contribution from the probability that two times are in the same forcing interval, and are therefore perfectly correlated. However, the directed forcing may also be correlated between forcing intervals, resulting in an additional term. Let p and q, respectively, be the probability that a social behavioral choice f made at position x at time t is 1 and -1. Then the expected value of the behavioral decision is $\phi(x,t) = E\{f\} = p - q$. The correlation between the forcing in two distinct social forcing intervals is

$$p^2 + q^2 - 2pq = \phi^2(x,t) , \tag{18}$$

where the first two terms of the left side of (18) correspond to the case in which forces in the intervals are both positive or both negative, and the third term represents the case where the force in one interval is positive while the other is negative. The social forcing autocorrelation is then

$$R_d(\tau) = \alpha^2 \frac{\lambda_s}{\lambda} \left[e^{-\lambda|\tau|} + (1 - e^{-\lambda|\tau|}) \frac{\lambda_s}{\lambda} \phi^2(x,t) \right] . \tag{19a}$$

The social forcing power spectrum is

$$S_d(\omega) = \sqrt{\frac{2}{\pi}} \alpha^2 \frac{\lambda_s}{\lambda} \left(\frac{2\lambda_r}{\lambda^2+\omega^2} \right) \left[1 + \left(\frac{\lambda_s}{\lambda} \phi(x,t) \right)^2 \right] + \sqrt{2\pi} \left(\alpha \frac{\lambda_s}{\lambda} \phi(x,t) \right)^2 \delta(\omega) , \tag{19b}$$

where $\delta(\omega)$ is the Dirac delta function.

The expression for the total forcing power spectrum (the general case, $U \neq 0$, proceeds similarly) is then

$$S_F(\omega) = \sqrt{\frac{2}{\pi}}\, c_1 \left(\frac{\lambda_r}{\lambda^2 + \omega^2}\right) + \sqrt{2\pi}\, c_2\, \delta(\omega),$$

$$c_1 = \sigma^2 \frac{\lambda_r}{\lambda} + \alpha^2 \frac{\lambda_s}{\lambda} - c_2, \qquad c_2 = \left(U + \alpha \frac{\lambda_s}{\lambda} \phi(x, t)\right)^2 . \tag{20}$$

Finally, substituting the parameters D, λ, γ, and Δx_s,

$$R_v(\tau) = \frac{\lambda^2(D + \Delta x_s \gamma) - \lambda(\gamma\phi(x, t))^2}{\lambda^2 - 1}\left[e^{-|\tau|} - \frac{1}{\lambda} e^{-\lambda|\tau|}\right] + (U + \gamma\delta\phi(x, t))^2. \tag{21}$$

The first term on the right side of (21) represents deviations from the mean due to the random walk and the intermittency of the social forcing. The second term is the square of the mean velocity at x, a contribution which does not vary with time delay (as long as the forcing is stationary). Equation (21) is valid for short times; the autocorrelation of velocity for individuals remaining within a stationary aggregation must be negative for some time lags (see Okubo 1986).

A potentially useful feature of the velocity autocorrelation is that it distinguishes movement characteristics inside and outside the aggregation, and at the interface between them (Fig. 1b). Statistics of movement based on the autocorrelation may therefore be applicable in characterizing animal behavior and determining aggregation parameters. The velocity autocorrelation (averaged over all individuals) measured in simulations agrees with that predicted by (21) for individuals in the interior of an aggregation, i.e., for $\phi = 0$ (Fig. 1b). This is expected since most individuals are in the interior most of the time in these simulations.

The time and space scales of individual movement decisions are typically small compared to those governing density fluxes. Taking advantage of this, (21) can be simplified by finding its limiting expression as the time and space scales of individual motion approach zero, $\lambda \to \infty$ and $\Delta x_s \to 0$,

$$R_v(\tau) = De^{-|\tau|} + (U + \gamma\phi(x, t))^2 . \tag{22}$$

Equation (22) shows that over the time and space scales of interest in group dynamics, individuals in a neighborhood experience a local mean velocity of $(U + \gamma\phi(x, t))$ in addition to the diffusive motion scaled by the diffusion coefficient, D. Thus, according to (22), the Eulerian equation for the flux of animal density due to the Lagrangian behavioral algorithm takes the form

$$\frac{\partial \rho}{\partial t} = D\frac{\partial^2 \rho}{\partial x^2} - \frac{\partial}{\partial x}[\rho(U + \gamma\phi(x, t))] . \tag{23}$$

In the next section, I complete the derivation of the Eulerian model by calculating an estimate for ϕ, the expected value of the social movement decision, as a function of the density distribution.

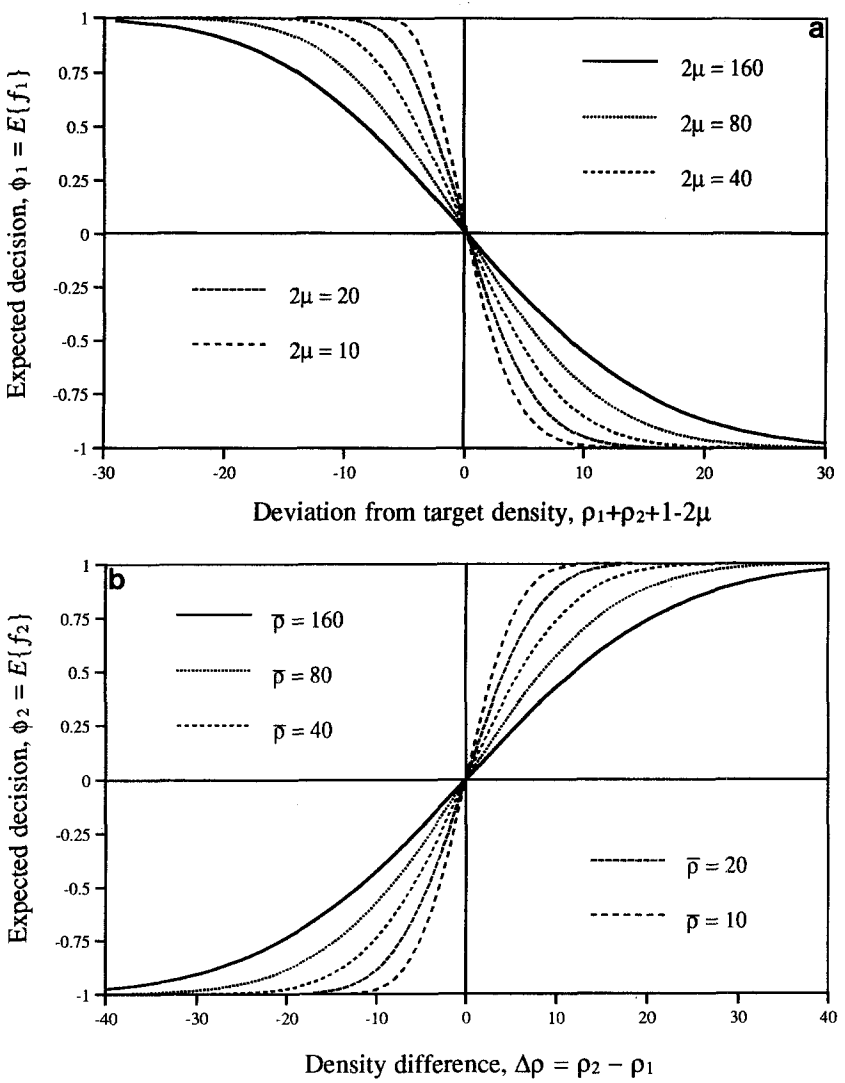

Fig. 2. **a** Expected value of the switching function for density, $\phi_1(\rho_1 + \rho_2, \mu) = E\{f_1(v_1, v_2)\}$, as a function of the expected deviation from target density, $\rho_1 + \rho_2 + 1 - 2\mu$, for several values of the target number of sensed individuals, 2μ. **b** Expected value of the switching function for density gradient, $\phi_2(\rho_1, \rho_2) = E\{f_2(v_1, v_2)\}$, as a function of the expected difference between numbers of neighbors on the right and on the left, $\Delta\rho = \rho_2 - \rho_1$, with constant total number of neighbors, $\bar{\rho} = \rho_1 + \rho_2$. **c** Expected social decision, $\phi(\rho_1, \rho_2) = E\{f(v_1, v_2)\}$, for values of ρ_1 and ρ_2 between 0 and 160, with target density $\mu = 40$. ϕ is antisymmetric about the axis $\rho_1 = \rho_2$; it is approximately equal to the product of the expected density switching behavior, ϕ_1, and the expected density gradient switching behavior, ϕ_2

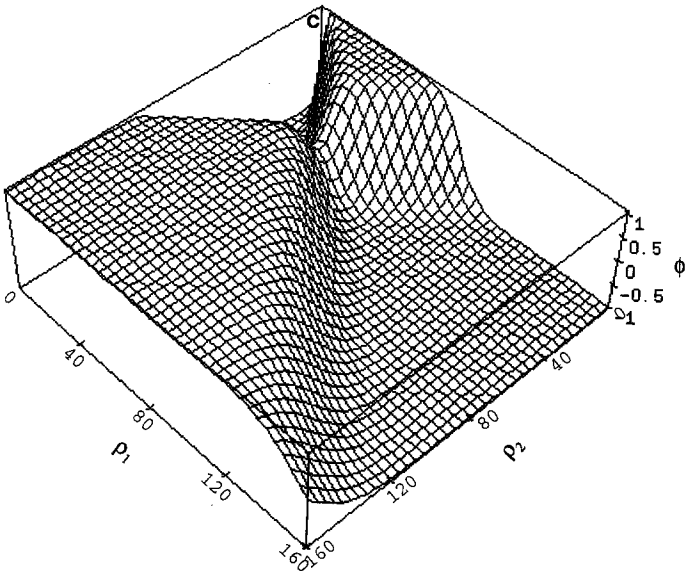

Fig. 2c

5 Pide aggregation model

The population flux due to social behavior at a position x is determined according to (23) by the function $\phi(x, t) = E\{f(x, t, v_1, v_2)\}$. ϕ can be expressed in terms of the joint probability density function, $c(v_1, v_2)$, of measuring v_1 and v_2 individuals, respectively in the unit intervals below and above a location x,

$$\phi(x, t) = \sum_{v_1=0}^{\infty} \sum_{v_2=0}^{\infty} c(v_1, v_2) f(x, t, v_1, v_2) \,. \tag{24}$$

Further progress requires an assumption about the nature of the joint probability density function, $c(v_1, v_2)$. There is no a priori theoretical reasoning which suggests an analytical expression for $c(v_1, v_2)$ as an outcome of the Lagrangian behavioral algorithms. However, a comparison of the mean and variance of bin densities in the stochastic simulation (Fig. 1c) suggests that, for some parameter values, a reasonable assumption might be that the distribution of individuals can be approximated as a set of Poisson points governed by the density distribution, ρ. If that is the case, then v_i, the number of individuals occurring in sampling domain i in any given observation, will obey a Poisson distribution, specified by the average sample number, ρ_i.

Formally, to be a set of Poisson points, the distribution of individuals must satisfy the following conditions (Papoulis 1984):

(*i*) the probability of v individuals being present in a sample from an interval, $[x_1, x_2]$, depends only on v, x_1, and x_2, for any x_1 and x_2;

(*ii*) the probabilities of samples v_n on n distinct intervals are independent; and
(*iii*) there is zero probability that a sample on a finite interval is infinite.

Conditions (*i*) and (*ii*) are not strictly satisfied in the Lagrangian simulation, since a large deviation in the number of individuals present in one interval may be correlated with a change in a neighboring interval. However, for parameters where the relative motion of individuals is highly random, these correlations may be found "empirically" in the Lagrangian simulations to be unimportant. For such cases, the consequences of the Poisson point assumption may give a good approximation to the joint probability density function.

Under the Poission assumption, the number of individuals sensed in the positive and negative directions, v_1 and v_2, are then independent,

$$c(v_1, v_2) = c_1(v_1)c_2(v_2). \tag{25a}$$

In (25a), c_1 and c_2 are the probability density functions for the number of individuals observed in sampling domains $\boldsymbol{d}_1$ and $\boldsymbol{d}_2$,

$$c_1(k) = e^{-\rho_1}\frac{\rho_1^k}{k!}, \qquad c_2(k) = e^{-\rho_2}\frac{\rho_2^k}{k!}, \tag{25b}$$

where the average sample numbers are

$$\rho_1(x,t) = \int_{\boldsymbol{d}_1} \rho(x',t)\,dx' = \int_{x-1}^{x} \rho(x',t)\,dx',$$

$$\rho_2(x,t) = \int_{\boldsymbol{d}_2} \rho(x',t)\,dx' = \int_{x}^{x+1} \rho(x',t)\,dx'. \tag{26}$$

Equations (25) and (26), together with (3), quantify the ability of individuals to determine whether they are above or below the target density ($\phi_1 = E\{f_1\}$) and detect the sign of the density gradient ($\phi_2 = E\{f_2\}$) for a given density distribution (Fig. 2). Using (24), the Eulerian equation for flux of animal density (23) can be stated explicitly, with the average behavioral decision, $\phi = E\{f\}$, written as a non-linear function of integral arguments ρ_1 and ρ_2, which are defined for all x and t (Fig. 2).

To summarize the developments in Sect. 3–5, the equation describing expected density flux in the Lagrangian model is a non-linear partial integro-differential equation (PIDE), (23), in which γ is the characteristic aggregation velocity derived from Lagrangian behavior parameters, ϕ is the local expected value, (24), of the behavioral decision, written as a function of the average number of neighbors in the sampling domains, (26), and the probability density functions of (25). U is an environmental advection velocity, and D a diffusivity calculated from Lagrangian parameters. This equation is based on an interpretation of the density distribution ρ as representing occurrences of individuals as Poisson points, an interpretation justified for particular choices of parameters by results of Lagrangian simulations.

A numerical solution (Fig. 3a) to (23) shows that the PIDE model qualitatively and quantitatively predicts the statistically stationary aggregation

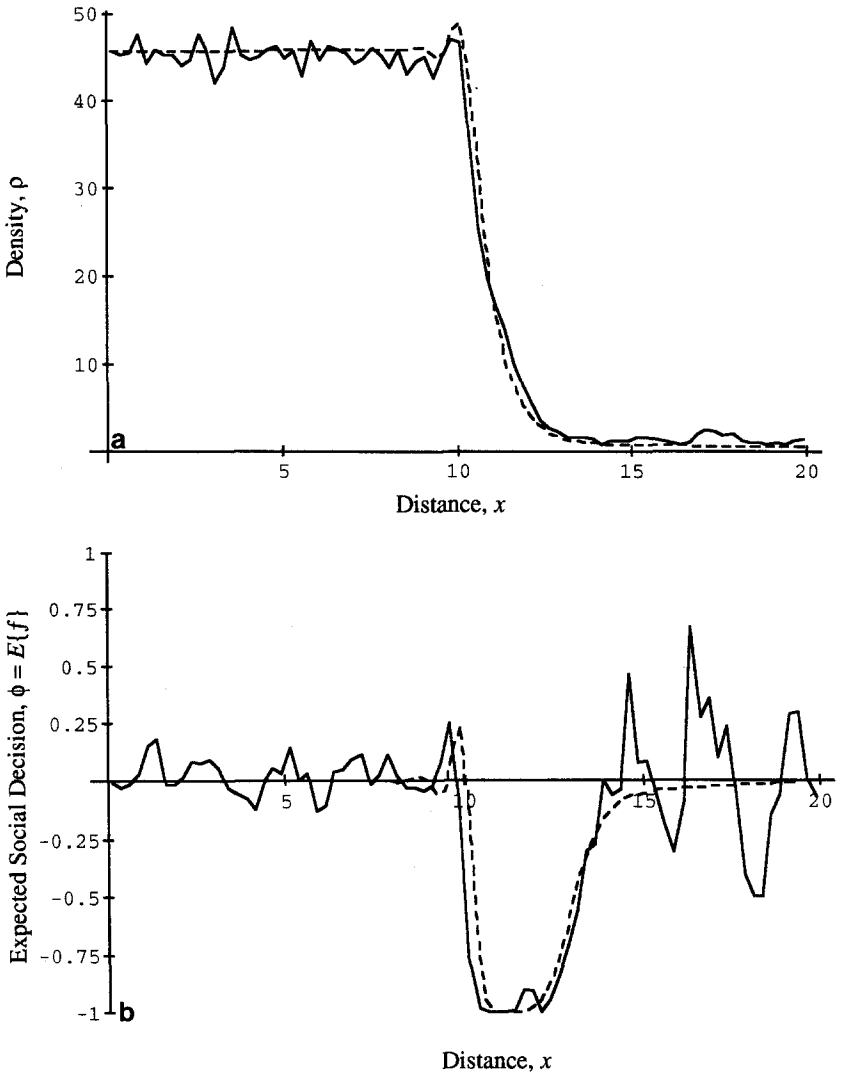

Fig. 3. **a** Expected density of the stochastic model (*solid*) and of the PIDE model (*dashed*), for a statistically stationary aggregation. Parameters are as in Fig. 1. The PIDE model accurately predicts both the density of individuals in the interior of the aggregation and the general shape of the density front. The peak at the edge of the density front is observed in both the stochastic and the PIDE models. It results from the spatial averaging that individuals perform in estimating local density. **b** Expected value of the social decision function, $\phi = E\{f(v_1, v_2)\}$, measured per bin in the stochastic model (*solid line*), and its approximation, $\phi(\rho_1, \rho_2)$, computed in the PIDE model with the Poisson process assumption (*dashed line*)

resulting from the stochastic model. This solution was computed for the spatial domain $0 \leqq x \leqq 20$, with no-flux boundary conditions. Both the density level inside the aggregation and the character of the swarm boundary are represented accurately. The average behavioral decision estimated using the

Poisson point assumption, ϕ, also agrees with the empirical $E\{f\}$, measured in the Lagrangian model (Fig. 3b). Forces due to social behavior act almost exclusively in a narrow band at the swarm boundary, and are small both in the interior and exterior of the aggregation. This is because within the boundary region, individuals have little uncertainty about the direction of the density gradient; the magnitude of ϕ is therefore close to unity throughout the interface. Density in the boundary region results from a balance of outwardly directed diffusive flux and inwardly directed aggregation flux. This balance produces a characteristic boundary distribution which decays exponentially as γ/D, giving roughly self-similar swarm structure when the number of individuals and target density are increased proportionately.

The results shown in Fig. 3 suggest that the continuum equation (23) is a useful approximation for statistically stationary stochastic aggregations. In Sect. 4, I compare the predictions of linear stability analysis and transient numerical solutions of (23) to unsteady dynamics of the Lagrangian aggregation model.

6 Linear stability and random initialization

Formation of aggregations from an initially uniform animal distribution is a common and important biological phenomenon, which can arise either through a spatially uniform "source" term or from temporal variations in tendencies to aggregate. For example, an aggregating life-stage can emerge from a non-aggregation one, as when fish or krill eggs and larvae, initially dispersed by advection, metamorphose into aggregating juveniles. Temporal variation in aggregation tendencies among animals occurs on a wide range of timescales: milli-seconds to seconds, as when krill or fish schools response to the presence of a predator; hours, as in animals which disperse at night and re-aggregate at dawn; and days or months, as in animals which aggregate in the course of annual reproductive cycles or seasonal migrations.

The initial stages of aggregation from a weakly perturbed uniform initial conditions can be investigated with linear analysis. Assume the density distribution is of the form

$$\rho(x) = \rho_{mean} + \rho' \sin(\pi k x) e^{st}, \quad \rho' \ll e_{mean} . \tag{27}$$

Substituting (27) into (23), taking advection U to be zero, and retaining only first order terms in ρ', the exponential growth rate for uniform initial condition for perturbations of wavenumber k is

$$s = -\pi^2 D k^2 + 2\gamma \rho_{mean} \frac{\partial \phi}{\partial \rho_1} (\cos(\pi k) - 1) , \tag{28}$$

where $\partial\phi/\partial\rho_1$ is evaluated at $\rho_1 = \rho_2 = \rho_{mean}$, and $\partial\phi/\partial\rho_1 = -\partial\phi/\partial\rho_2$. From (31), it is clear that the exponential growth rate s of a small perturbation can be positive only if $\partial\phi/\partial\rho_1$ is negative; this is possible only for $\rho_{mean} < \mu$ (Fig. 4).

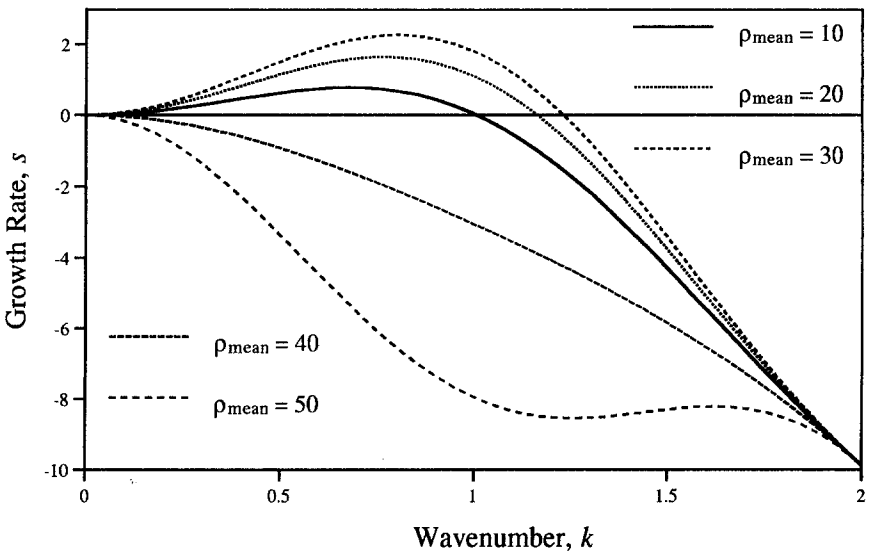

Fig. 4. Growth rates s of small sinusoidal perturbations of wavelength $2/k$ for the parameters $\mu = 40$, $\gamma = \sqrt{2}/4$, and $D = 1/4$, for a range of initial densities, ρ_{mean}

Thus a uniform state with density above the target density is always stable. Below the target density, there is a range of unstable wavenumbers. Neither the range of wavenumbers of growing disturbances nor the wavenumber of the fastest growing mode appear strongly dependent on initial density, as long as the initial density is below the target density. This suggests that the length scale of aggregations arising out of initially uniform distributions is, to some extent, fixed by the sensing capacity of the animals, in the form of the sensing distance. However, the growth rate of the fastest growing disturbance does vary with initial density, reaching a maximum in the vicinity of $\rho_{mean} = 30$. This suggests that animals may have difficulty forming aggregations when initial densities are too low.

Predictions of linear stability analysis are confirmed by transient density distributions in the Lagrangian and PIDE models with 512 individuals initially uniformly distributed at a density of $\mu/2$ (Fig. 5). In the Eulerian simulation, white noise perturbation was superimposed on the initial density distribution in the PIDE model, such that the RMS deviation was 1.5% of the initial density. The stochasticity resulting from a finite number of individuals made a perturbation of the stochastic model unnecessary. In both models, the initially uniform distributions coalesce into small groups, regularly spaced with a wavenumber $k \approx 0.8$. This value agrees with the predicted fastest growing wavenumber (Fig. 4).

As deviations from initial conditions become large, the aggregation process continues via the successive amalgamation of small groups into larger ones, until a small number of well-separated groups remain (Fig. 5). In later

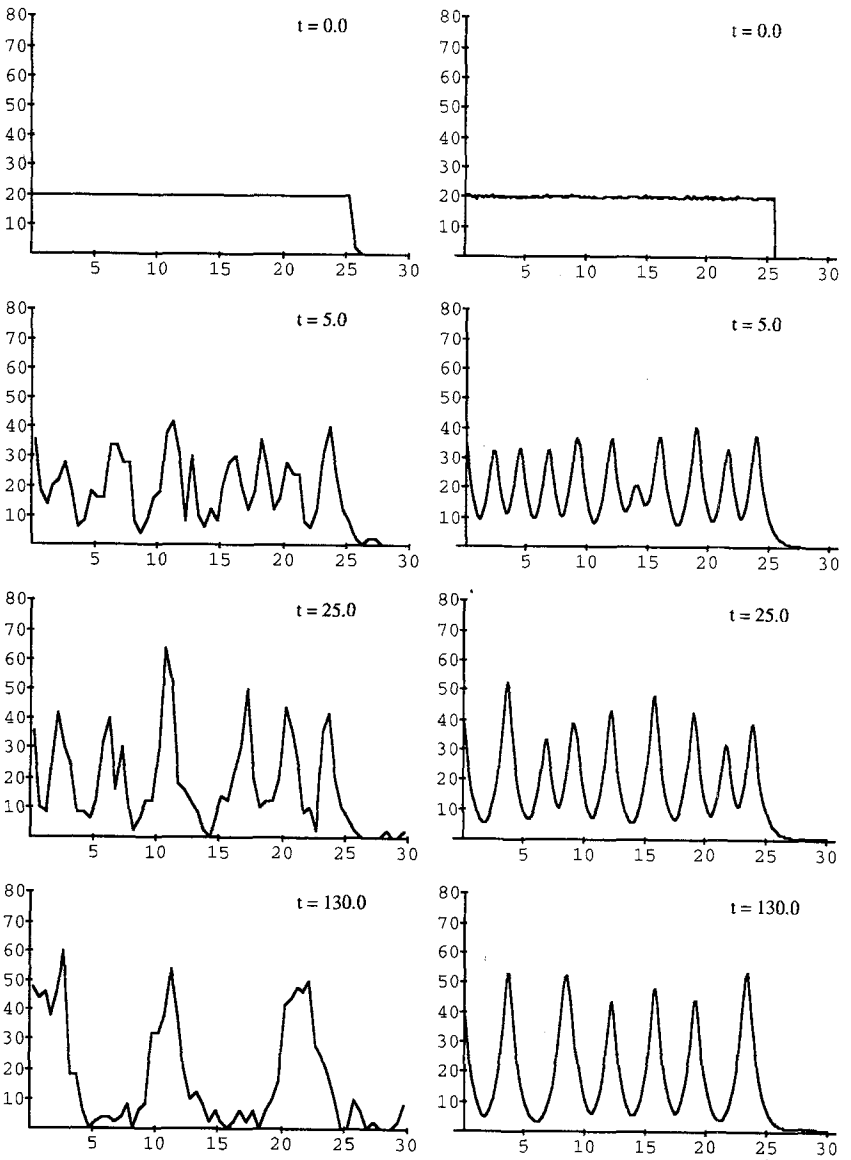

Fig. 5. Sequence of instanteneous density distributions resulting from an initial distribution of $\rho = \mu/2 = 20$ in the stochastic model (*left column*) and the PIDE model (*right column*). The PIDE model was purturbed with white noise with an RMS intensity of 1.5% of the initial density. As predicted by linear stability analysis, the initial distribution is unstable. Aggregation proceeds in amalgamation of groups. The aggregations formed in the first correspond to a wavenumber, k, of roughly 0.8, consistent with the predictions of linear stability analysis (Fig. 4). Coalescence proceeds more slowly in the PIDE model than in the stochastic model, where random fluctuations can result in drift of groups of individuals and in transient shifts of individuals within groups

stages, amalgamation proceeds more rapidly in the stochastic model than in the PIDE model. In the PIDE model, a series of almost perfectly balanced groups form very slowly changing or steady density distributions. In the stochastic model, such long-term balances are unlikely because of the continuous perturbation inherent in the random movement of individuals. In the presence of continual random perturbation, for example by a random advective field, coalescence might continue at a rapid rate in the PIDE model as well.

Discussion and summary

Aggregation of animals into large social groups is a ubiquitous and important phenomenon in a diverse array of biotic settings. For example, fish and large zooplankton such as Antarctic krill (*Euphausia superba*) form schools and swarms in marine habitats, wildebeests and other large mammals form herds in terrestrial habitats, and insects such as locusts form reproductive or migratory aerial aggregations. The processes determining animal distributions in these species have many obvious differences. However, these taxa all share the characteristic that, while individual behaviors ultimately determine group properties, dynamics at the levels of the individual and of the group occur on very different spatial and temporal scales. At the larger spatio-temporal scales characterizing group dynamics, Lagrangian models of socially interacting animals are computationally cumbersome and analytically inter-actable. Eulerian models, on the other hand, are efficient descriptions of animal distributions at large spatio-temporal scales, but do not explicitly represent social interactions. These difficulties motivate a dual approach, in which animal distributions at large-scales are investigated with Eulerian models that are derived directly from Lagrangian aggregation models with specific microscopic properties.

In this paper, I have examined a Lagrangian (individual-based) aggregation model of animals whose movements are determined by their attempts to attain a species-specific "target" density of conspecifics. The underlying assumption is that animals respond only to conspecifics within a limited sensory range. Swarm members thus have limited knowledge of the spatial distribution of neighbors. The model demonstrates that limitations on information possessed by individual members about the swarm as a whole, together with decentralized control of a group of autonomous, non-cooperating individuals, have important consequences for the dynamics of swarm formation and maintenance. For example, despite the fact that all individuals seek the same target density the model predicts that animal densities are higher than the target density. Nearly all individuals are therefore unable to locate the appropriate density of conspecifics. This suggests that some desirable group properties, such as optimal density, may not always be feasible as the outcome of selection on individual behavior. Other consequences of decentralized control and sensory limitations may include lack of the coherence in large swarms whose spatial extent is much larger than the sensory distance of

individuals, i.e., an aggregation much larger than this distance may be relatively fragile, whereas an aggregation of that size or smaller may be relatively cohesive in the face of internal and external disturbances. Sensing range also appears to be the most important determinant of the size of aggregations arising from uniformly low initial conditions. Thus the maximum distance at which neighbors can be detected may be a useful standard by which to gauge an aggregation's "dynamical" size. The direct effects of aggregation behavior may be most evident at scales comparable to the sensing range, but may be dominated at larger scales by other physical and biotic effects.

From a more general theoretical perspective, I argued that in deriving an Eulerian expression for the animal density flux, a narrower and more specific interpretation of animal density is needed for density-dependent Lagrangian behavior than in the more familiar density-independent case. In particular, most Lagrangian algorithms for an individual's response to neighbors can be expressed as a response function to the number of neighbors observed within each of several spatial subdomains. Because of non-linear interactions inherent in density-dependent aggregation behavior, calculation of the flux requires that density must be interpreted in a way that specifies higher order moments of samples within and between subdomains. The resulting Eulerian models will in general take the form of non-linear partial integro-differential equations (PIDE's), with integral terms corresponding to each subdomain. These equations may be linearized for analysis, or solved numerically in their complete form with greater efficiency at large spatial and temporal scales than the underlying Lagrangian models.

In the present case, the key assumption in making the continuum approximation is that the number of conspecific neighbors sensed "to the right" and "to the left" of each focal individual are independent with Poisson probability density distributions, i.e., at any given observation, individuals are distributed as Poisson points. The likelihood of observing a given number of neighbors at a chosen location is then specified by integrals of the expected density distribution within the entire sensed range of an individual at that location. The Poisson assumption makes it possible to construct a function estimating the frequency of alternative behavioral decisions at each position within the aggregation and the resulting expected flux of individuals.

The Poisson distribution of the neighbors is not an assumption of the individual behavior simulation. However, it turns out that the Eulerian approximation and the individual-based stochastic simulation agree remarkably well, as long as individual animal motions have a sufficiently large random component. Linear stability analysis of the density flux equation shows that an uniform distribution is unstable only if the initial density is below the target density, and then only for disturbances of sufficiently long wavelengths. In this unstable range, the most rapidly growing wavelength is only weakly dependent on initial density. Linear analysis correctly predicts the wavelength of the initial swarming pattern in both the stochastic model and the full Eulerian equation.

One of the values of a continuum approach is its ability to predict characteristic group properties from a small number of parameters. The analysis presented in this paper yields a characteristic aggregation velocity and a diffusion constant based on the parameters of individual motion in the Lagrangian model. These two parameters alone appear in the Eulerian model, and are sufficient to predict the swarm dynamics and equilibrium aggregation shapes which arise in the Lagrangian model. The analysis also suggests that comparisons of the velocity autocorrelations of individuals in the interior, at the boundary and outside aggregations may be useful in characterizing social behavior algorithms and estimating parameters.

When comparing the stochastic simulation with the continuum model in terms of successive merging of dispersed swarms, it is interesting that while random fluctuations in animal density in the two models initially display similar rates of coalescence into swarms, later stages of aggregation proceed substantially faster for the individual simulation than the continuum model. This appears to be because the continuum model forms chains of finely balanced aggregations; in the absence of environmental distrubances, these swarms merge only very slowly if at all. Stochastic fluctuations in the individual-based model make such balanced distributions impossible.

Overall, it appears that useful insight about continuum properties can be gained by approximating detailed social behavioral algorithms with PIDE's. The obvious next step would include more complex behaviors in multiple dimensions that involve interactions between species, or between one species and a heterogeneous environment.

Acknowledgments. I thank S. Levin, A. Okubo, T. Powell, C. Greene, and T. Daniel for support and encouragement. P. Kareiva, L. Edelstein-Keshet, C. Jordan, and three anonymous reviewers gave thoughtful comments on the manuscript which improved it greatly. This work was supported in part by N.S.F. Grant BSR-8806202 and Hatch Grant NYC-183430 to S. Levin, by O.N.R. Grant N00014-92-J-1527 to H. Caswell. The author also gratefully acknowledges the support of an Izaak Walton Killam Memorial Fellowship.

References

Aiko, I.: A simulation study on the schooling mechanism in fish. Bull. Jpn. Soc. Sci. Fish **48**, 1081–1088 (1982)

Alt, W.: Models for mutual attraction and aggregation of motile individuals. Lect. Notes Biomath. **57**, 33–38 (1985)

Cohen, D. S., Murray, J. D.: A generalized diffusion model for growth and dispersal in a population. J. Math. Biol. **12**, 237–49 (1981)

Heppner, F., Grenander, U.: A stochastic nonlinear model for coordinated bird flocks. In: The Ubiquity of Chaos (ed.) Krusna, S. Washington, DC: AAAS Publications, 1990, pp 233–238

Huth, A., Wissel, C.: The movement of fish schools: a simulation model. In: Biological Motion (eds.) Alt, W., Hoffmann, G., Lect. Notes Biomath. vol. 89, pp 577–590. Berlin Heidelberg New York: Springer 1990

Huth, A., Wissel, C.: The simulation of the movement of fish schools. J. Theor. Biol. **156**, 365–385 (1992)

Kawasaki, K.: Diffusion and the formation of spatial distributions. Math. Sci. **16**(183), 47–52 (1978)

Levin, S. A.: Random walk models and their implications. In: Hallam, T. G., Levin S. A. (eds.) Mathematical ecology. Biomathematics, vol. 17, pp 149–154. Berlin Heidelberg New York: Springer 1986

McFarland, W. N., Moss, S. A.: Internal behavior in fish schools. Science **156**(3772), 260–262 (1967)

Okubo, A.: Dynamical aspects of animal grouping: swarms, schools, flocks and herds. Adv. Biophys. **22**, 1–94 (1986)

Papoulis, A.: Probability, random variables, and stochastic processes. New York: McGraw-Hill 1984

Pfistner, B., Alt, W.: A two dimensional random walk model for swarming behavior. In: Biological Motion (eds.) Alt, W., Hoffmann, G., Lect. Notes Biomath. vol. 89, pp 564–565. Berlin Heidelberg New York: Springer 1990

Sakai, S.: A model for group structure and its behavior. Biophysics **13**, 82–90 (1973)

Strand, S. W., Hamner, W. M.: Schooling behavior of Antarctic krill (*Euphausia superba*) in laboratory aquaria: reactions to chemical and visual stimuli. Mar. Biol. **106**, 355–359 (1990)

Suzuki, R., Sakai, S.: Movement of a group of animals. Biophysics **13**, 281–282 (1973)

Turchin, P.: Population consequences of aggregative movement. J. Animal Ecol. **58**, 75–100 (1989)

Warburton, K., Lazarus, J.: Tendency-distance models of social cohesion in animal groups. J. Theor. Biol. **150**, 473–488 (1991)